Electronic Supplementary Information

Revealing stable geometries and magic clusters of hexagonal boron nitride in nucleation of chemical vapor deposition growth on Ni(111)/Cu(111) surfaces: A theoretical study

Hongxia Zhu,[a] Xiaolei Zhao,[b] Huanhuan Li,[a] Ruiqi Zhao,*[, a,c]

[a]Henan Key Laboratory of Materials on Deep-Earth Engineering, School of Materials Science and Engineering, Henan Polytechnic University, Henan 454003, China

[b]College of Chemistry and Chemical Engineering, Henan Polytechnic University, Henan 454003, China

[c]College of Chemistry and Molecular Engineering, Beijing National Laboratory for Molecular Sciences, Peking University, Beijing 100871, China

Contents:

1. Adsorption sites, tests of stable configurations and different functionals.

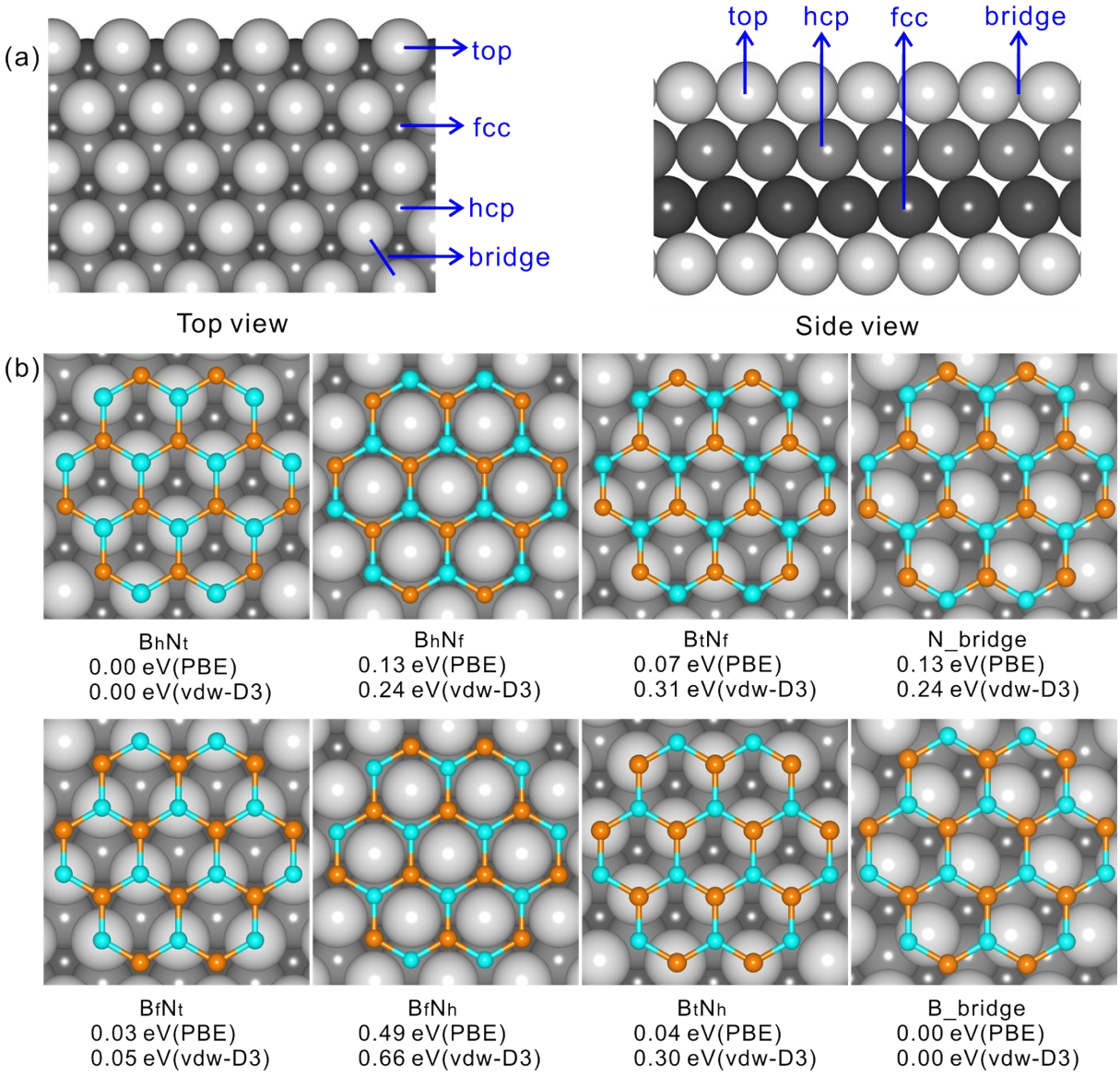

Fig. S1 (Color on line) (a) Adsorption sites of top, hcp, fcc and bridge seen from top (left) and side (right) views. (b) Eight configurations and relative energies obtained from PBE and vdw-D3 of $(BN)_{12}$ on Ni(111) with different adsorption sites. The configurations are named with elements and the adsorption sites docked by B and N. The relative energies compared to B_hN_t are also listed. The orange, blue and grey balls represent boron, nitrogen and Ni atoms, respectively. The color of metal atoms becomes darker in the order of ascending depth to highlight the difference of adsorption sites occupied by B and N atoms. The configurations with N_bridge and B_bridge turn into B_hN_f and B_hN_t respectively after full relax.

2. Relaxed configurations of BN clusters (*n* = 26-28) @Ni(111) surface.

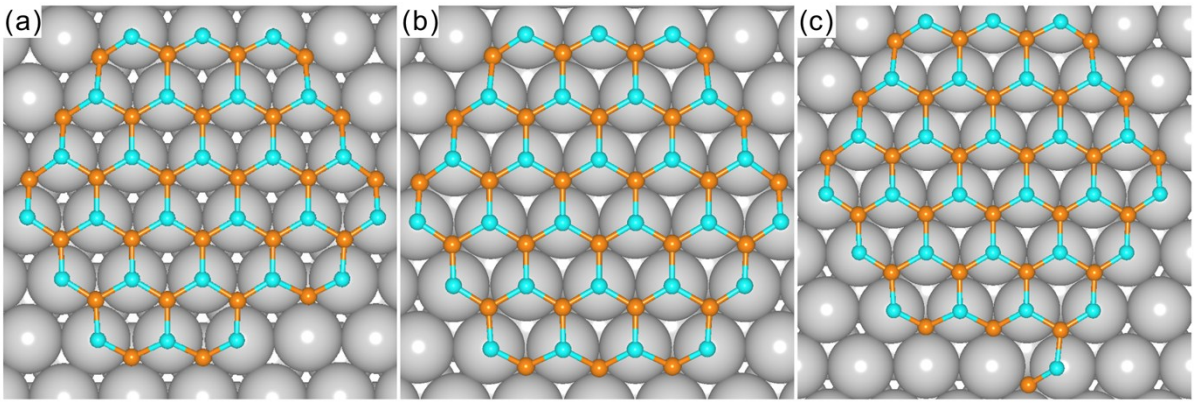

Fig. S2 (Color on line) Relaxed configurations of BN clusters@Ni(111) surface: (a) *n* = 26, (b) *n* = 27, (c) *n* = 28. The configurations of $(BN)_{26}$ and $(BN)_{27}$ are composed with 18 and 19 hexagons, respectively.

3. Simulated STM images of magic clusters of $(BN)_{12}$ and $(BN)_{27}$ on Ni(111) surface.

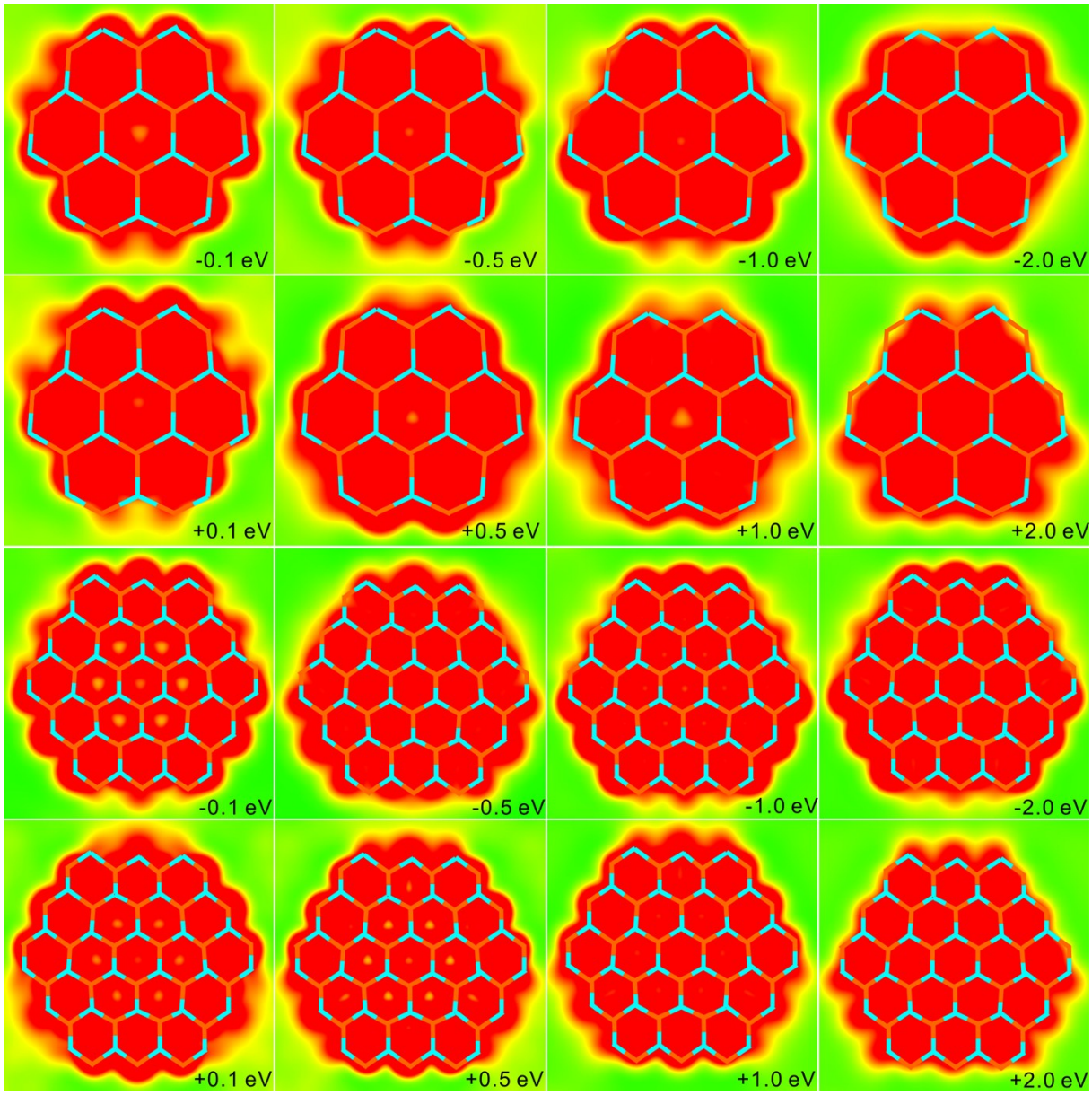

Fig. S3 (Color on line) Simulated STM images of magic clusters of $(BN)_{12}$ and $(BN)_{27}$ on Ni(111) surface at different scanning conditions.

4. Top views of free-standing clusters (*n* = 6-13) with the same geometries of BN clusters in Fig. 2d.

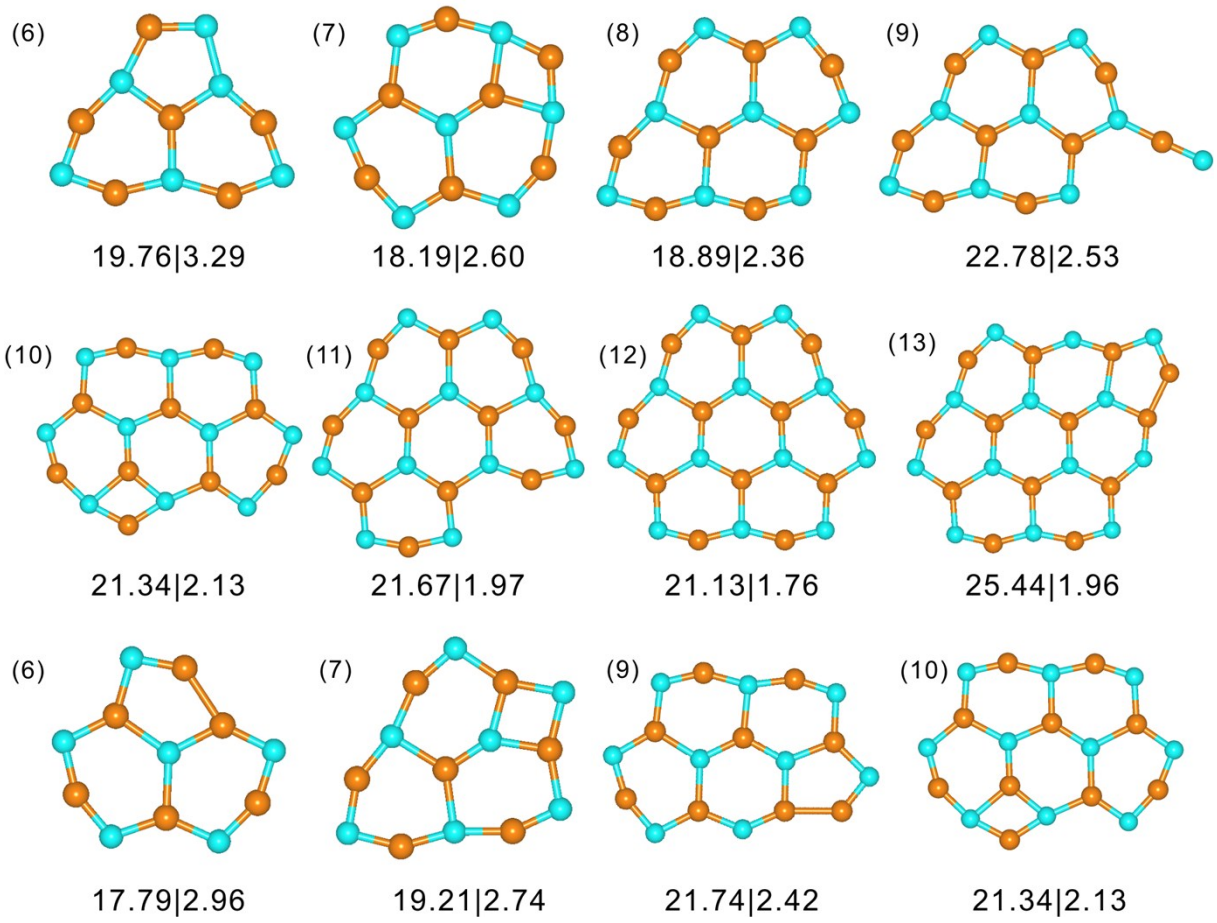

Fig. S4 (Color on line) Top views of relaxed configurations of free-standing $(BN)_n$ clusters with n = 6-13. The configurations are listed in the same order as those shown in Fig. 2d. The formation energies and relative chemical potentials of each BN cluster ($E_f|\Delta\mu$, eV) are also listed under each panel.

5. Binding energies per BN pair in each BN cluster with n = 6-13.

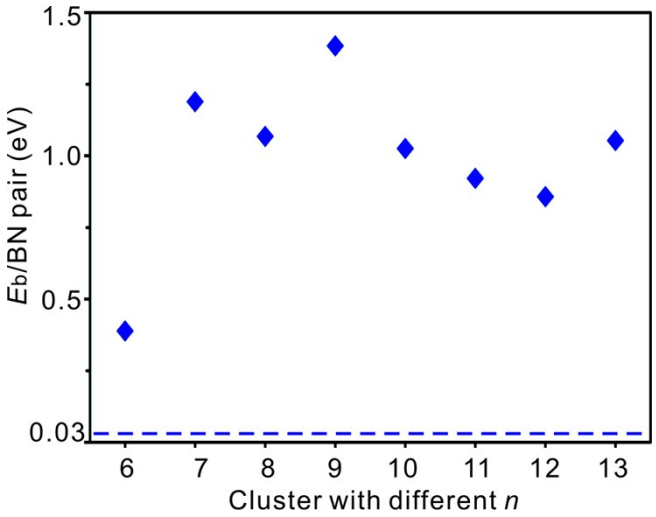

Fig. S5 (Color on line) Binding energies (eV) per BN pair in each BN cluster with n = 6-13. The binding energy of BN film on Ni(111) surface is also listed for comparison.

6. Top views of various isomers of $(BN)_{12}$ on Ni(111) and corresponding free-standing structures.

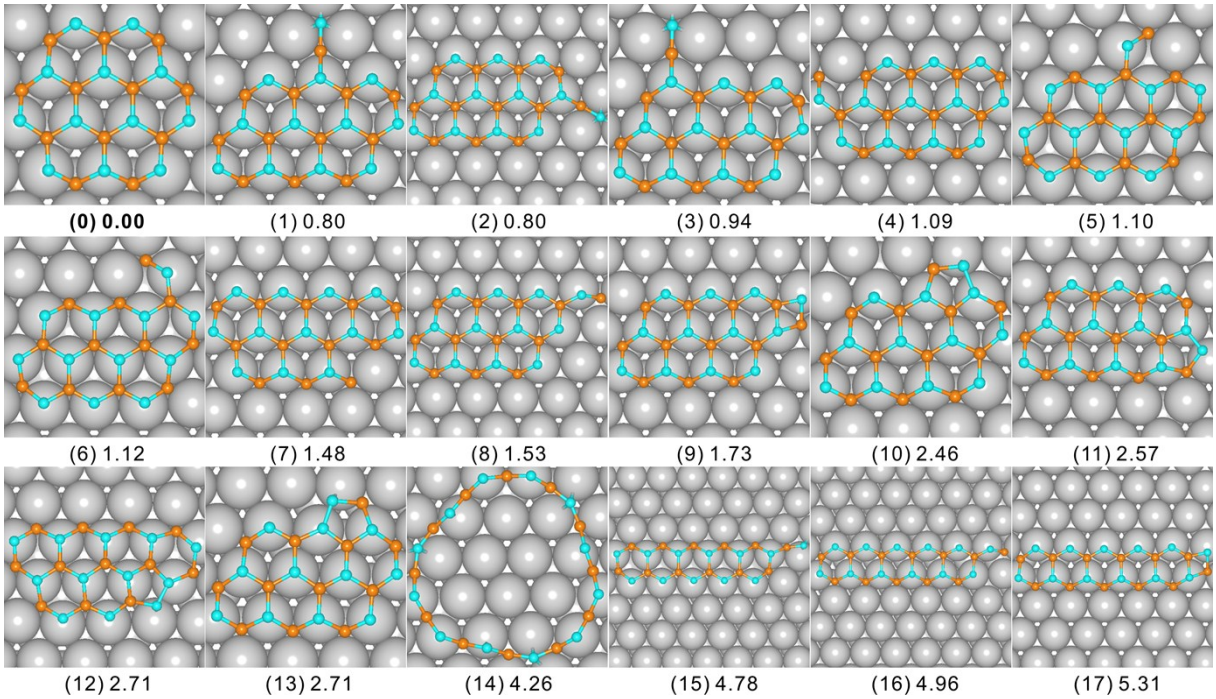

Fig. S6 (Color on line) Top views of relaxed configurations of various isomers, $I_{(12,\ i)}$ on Ni(111) surface. The isomers are arranged in order of ascending energies and only the number, *i*, is listed to identify each panel. The energy of the most stable structure (12, 0) is set as zero. The relative energy (eV) compared to that of $I_{(12,\ 0)}$ is also listed under each panel.

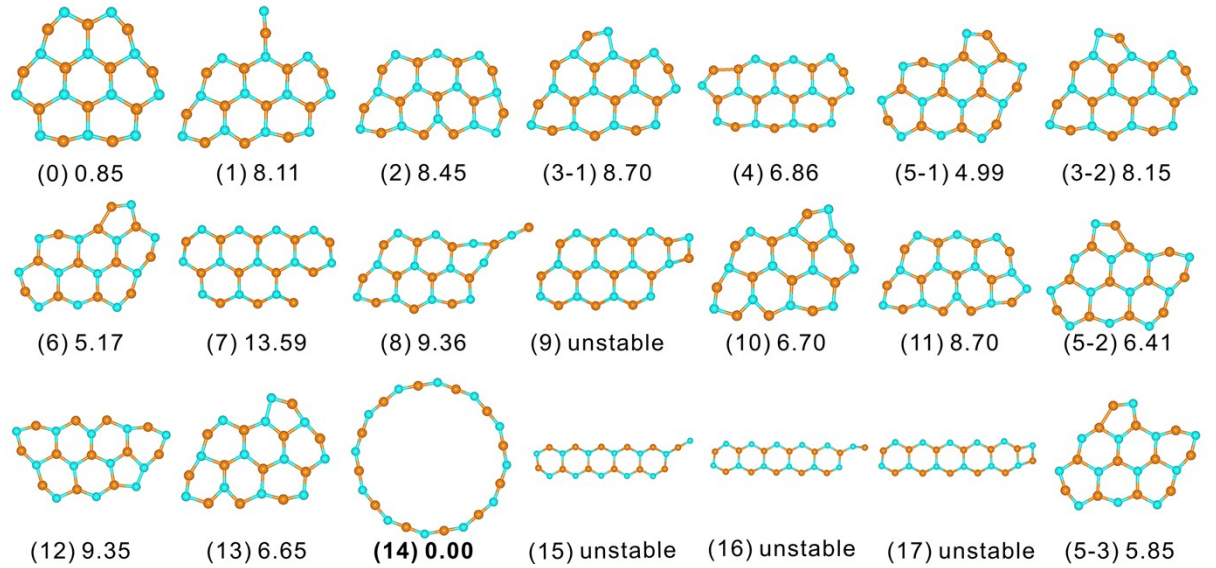

Fig. S7 (Color on line) Top views of relaxed configurations of free-standing $(BN)_{12}$ arranged in the same order as those on Ni(111) (Fig. S6). The energy of the ring-like structure is set as zero. The relative energy (eV) and the number, *i* is also listed under each panel.

7. Side views of relaxed configurations as well as top and cross-section views of differential charge densities of the magic cluster, $(BN)_{12}$ with different adsorption sites.

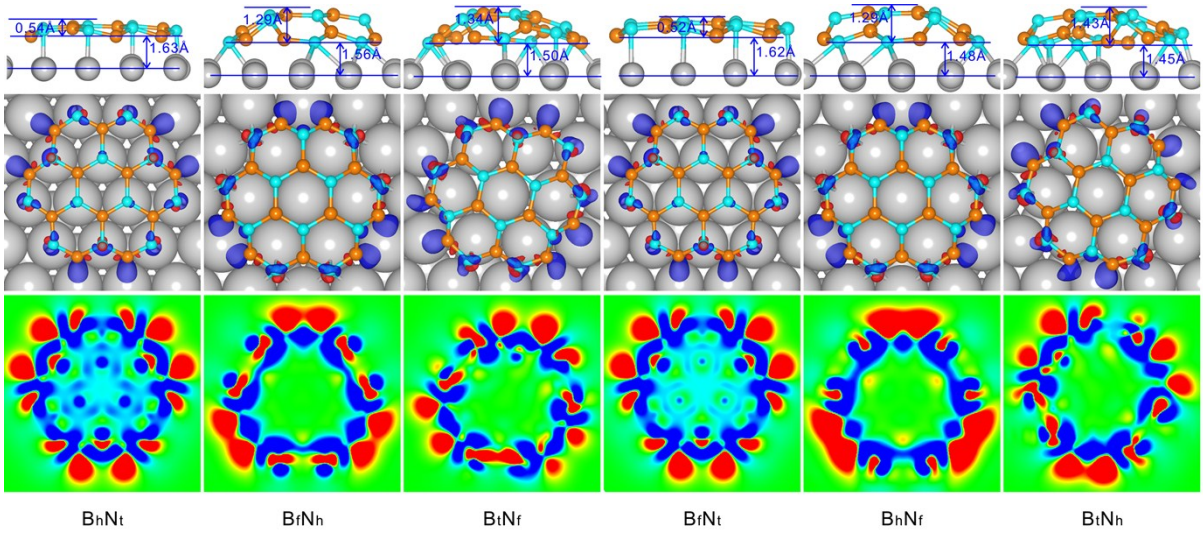

Fig. S8 (Color on line) (From top to bottom) Side view of the relaxed configurations, top and cross-section of the differential charge densities of $(BN)_n$ clusters (n = 12) on Ni(111): (a) B_hN_t, (b) B_fN_h, (c) B_tN_f, (d) B_fN_t, (e) B_hN_f, and (f) B_tN_h. The isosurface and electron distribution in slice view are 0.013 eÅ^{-3} and [-0.004, 0.004], respectively. Blue and red represent the regions of electron accumulation and depletion, respectively. The subscript letter h, t, and f indicates different adsorption sites, hcp, top, and fcc, respectively. The configuration B_hN_t is the most stable one. The deformations along z directions are also listed.

8. Side, top and cross-section views of differential charge densities of BN film, ring-shaped as well as magic geometries of $(BN)_{12}$ on Ni(111) surface.

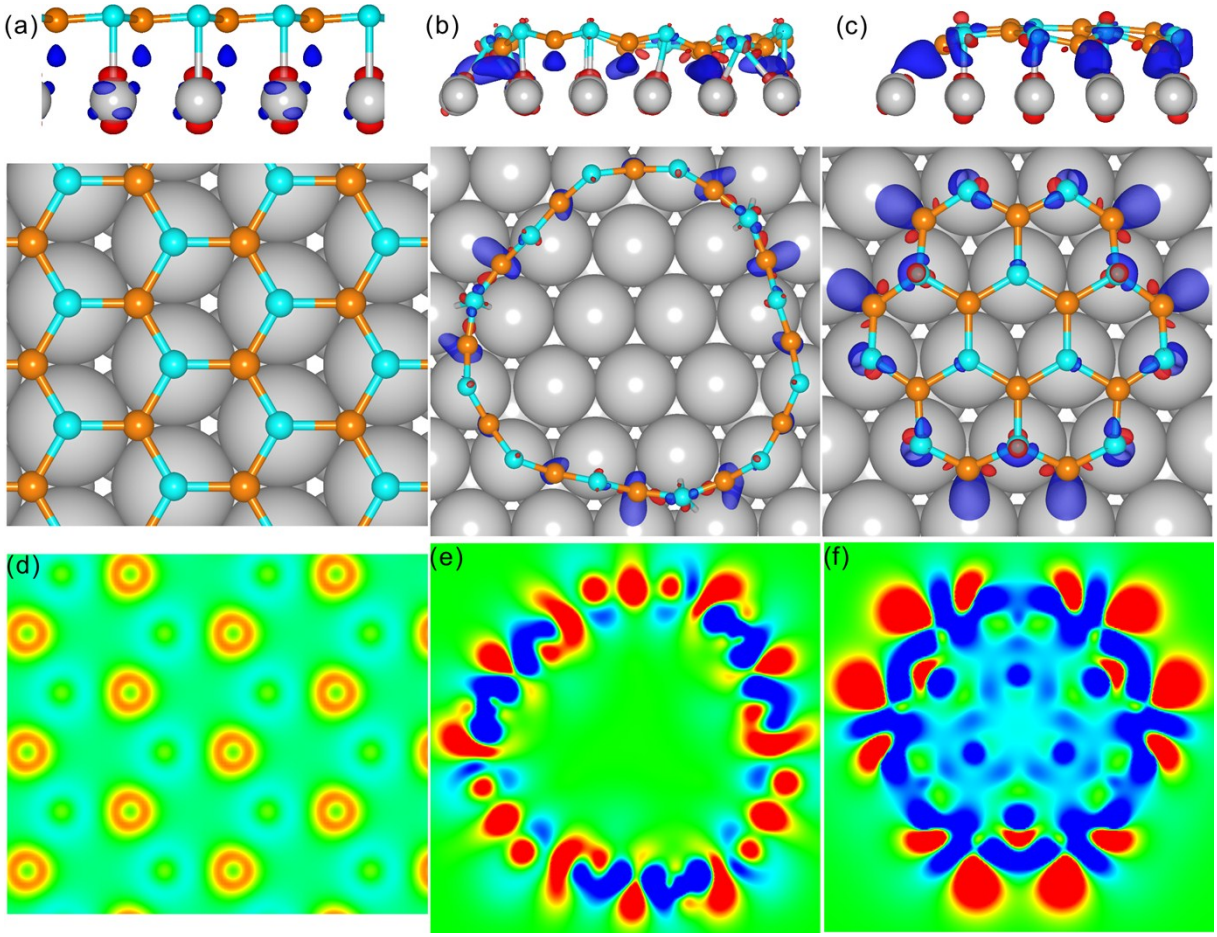

Fig. S9 (Color on line) (a-b) Side & top views and (d-f) cross-section views of the differential charge densities of BN film, ring-shaped as well as magic geometries of $(BN)_{12}$ on Ni(111) surface. The isosurface and electron distribution in slice view are 0.013 eÅ^{-3} and [-0.004, 0.004], respectively. Blue and red represent the regions of electron accumulation and depletion, respectively.

9. Bader charge analyses of free-standing BN film, ring-shaped and honeycombed BN clusters.

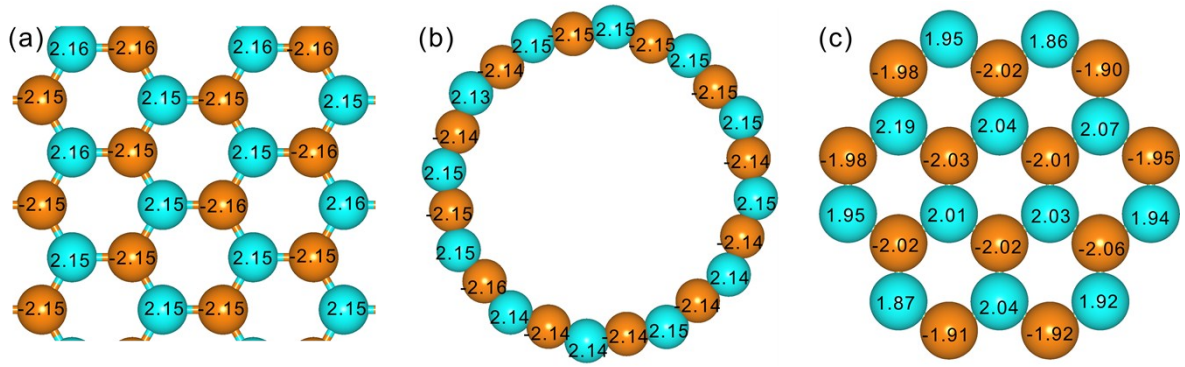

Fig. S10 (Color online) Bader charge analyses of free-standing BN film (a), ring-shaped (b) and honeycombed (c) BN clusters.